Nano Energy 71 (2020) 104638

Contents lists available at ScienceDirect

Nano Energy

journal homepage: http://www.elsevier.com/locate/nanoen

Communication

# Superstable copper nanowire network electrodes by single-crystal graphene covering and their applications in flexible nanogenerator and light-emitting diode

Jianwei Wang [a,c,1], Zhihong Zhang [b,1], Shujie Wang [c,1], Ruifeng Zhang [a], Yi Guo [b], Gang Cheng [c], Yuzong Gu [a], Kaihui Liu [b,*], Ke Chen [a,**]

[a] Physics Research Center for Two-Dimensional Optoelectronic Materials and Devices, Institute of Micro/Nano Photonic Materials and Applications, School of Physics and Electronics, Henan University, Kaifeng, 475004, China
[b] State Key Lab for Mesoscopic Physics and Frontiers Science Center for Nano-optoelectronics, International Center for Quantum Materials, Collaborative Innovation Center of Quantum Matter, School of Physics, Peking University, Beijing, 100871, China
[c] Key Laboratory for Special Functional Materials of Ministry of Education, Henan University, Kaifeng, 475004, China

ARTICLE INFO

*Keywords:*
Single-crystal graphene
Chemical vapor deposition
Copper nanowire
Super stability
Flexible transparent electrodes

ABSTRACT

Copper nanowires (CuNWs), with excellent electronic properties and high cost-effectiveness, have tremendous potential in the field of transparent conductive electrodes for flexible electronics, large touch screen display and triboelectric energy harvesters, while their vulnerability to oxidation in air has impeded possible practical applications. Fortunately, it has been recognized that graphene encapsulation of CuNWs is capable of protecting CuNWs. However, neither self-assembled reduced graphene oxide nor chemical vapor deposition-grown polycrystalline graphene coatings can guarantee full protection to CuNWs, due to their ubiquitous voids, grain boundaries and wrinkles that allow water and oxygen molecules to pass through and result in the accelerated electrochemical corrosion at the graphene-copper interface, especially under folding conditions. Herein, we demonstrate a sandwich-structured single-crystal graphene/copper nanowire network/UV-curable resin (SCG/CuNW/UVR) composite film with ultrahigh electronic performance stability. The SCG/CuNW/UVR electrode exhibits a good optical and electrical performance (~19 Ω $sq^{-1}$ under 84.3% transmittance), excellent mechanical robust and remarkably high oxidation resistance ($\Delta R/R_0 < 0.2$ within 180 days), in sharp contrast with the bare CuNWs ($\Delta R/R_0 > 1$ after 1 day) and polycrystalline graphene-covered CuNWs counterparts ($\Delta R/R_0 > 1$ after 7 days). Furthermore, the SCG/CuNW/UVR electrodes can replace indium tin oxide (ITO) electrodes to construct the triboelectric nanogenerators (TENG) and quantum dot light emitting diodes (QLED), comparable to the flexible commercial ITO counterparts. The fabrication of such high-performance SCG/CuNW/UVR electrode is facile to be scaled-up with low cost, providing the feasibility for industrial applications of flexible ITO-free electronic and optoelectronic devices.

## 1. Introduction

Emerging technologies for flexible, smart and wearable energy devices raise a high demand on transparent conductive electrodes (TCEs) [1–3]. Indium tin oxide (ITO) as a most common transparent electrode material is facing a gradual shrinking space in the applications of flexible display, touch screen, light emitting diodes and triboelectric energy generators, *etc*, because of its intrinsic brittleness, toxicity and rising production cost [4,5]. Therefore, tremendous efforts have been made to exploit novel TCE materials such as metal nanowires [6–12], graphene [13–15], carbon nanotubes [16–18] and conductive polymers [19,20] in the recent years. Silver nanowires with excellent conductive performance and mechanical flexibility have become an alternative candidate for ITO [21–24], but they are very expensive due to the scarcity of the mineral resources. Copper nanowires (CuNWs) have comparable electrical conductivity (94.6% of Ag) but more significant economic benefits

* Corresponding author.
** Corresponding author.
*E-mail addresses:* khliu@pku.edu.cn (K. Liu), kchen@henu.edu.cn (K. Chen).
[1] These authors contribute equally to this work.

https://doi.org/10.1016/j.nanoen.2020.104638
Received 13 January 2020; Received in revised form 11 February 2020; Accepted 18 February 2020
Available online 26 February 2020

(1000-times more abundant and 9% price of Ag) [25,26]. However, the severe Cu oxidation in air, causing rough surface and degraded electrical conductivity of CuNWs, has impeded their practical applications in TCEs.

In order to prevent Cu oxidation, most of the researches have been focused on encapsulation of CuNWs with diverse coatings such as metals, polymers, oxides, amorphous carbon [27–29], *etc*. Nevertheless, such surface passivation coatings could decrease the transmission and conductivity of the CuNW network, due to the intrinsic light absorption or scattering, as well as the enhanced electron-surface scattering and contact resistance of CuNWs. Graphene has naturally stimulated the interests in transparent electrodes because of its ultrahigh conductivity, excellent optical properties, as well as high chemical impermeability [30–34]. The critical role of graphene integrated with CuNWs is not only to serve as a transparent conductor but also to protect Cu from harsh environments [35–37]. In this context, reduced graphene oxide (rGO) sheet and polycrystalline graphene (PG) films grown by chemical vapor deposition (CVD) method have been applied to cover the CuNWs to improve their stability [38–41]. Unfortunately, both solution-processed rGO sheets and CVD-grown graphene layers are generally of abundant voids and intrinsic defects such as domain boundaries, vacancies and wrinkles [37,42]. These voids and defects allow small corrosive molecules (*e. g.* $O_2$ and $H_2O$) to penetrate through and thus result in the oxidation of CuNWs and the increase of their junction resistance.

Unlike rGO and polycrystalline graphene, single-crystal graphene (SCG) is highly impermeable, conductive and strong owing to its nearly perfect lattice. Large-area SCG films have been epitaxially grown on Cu (111) substrate by CVD method [43–46]. However, to date the high-efficiency transfer of SCG onto the rough and porous surface of CuNW network remains inaccessible. Herein, we prepared a SCG-stabilized CuNW network electrode by a layer-by-layer (LbL) coating approach, which includes: (*i*) the large-area SCG film was grown on single-crystal Cu(111) transformed from industrial polycrystalline Cu foils; (*ii*) the sandwich-structured graphene/CuNW/resin composite film was prepared by spray coating of CuNWs on SCG film, followed by a blade coating of UV-cured resin (UVR, Norland NOA 63); (*iii*) the Cu foil was etched via wet chemistry method. The LbL coating technique can avoid the extra defects and even micro-cracks of graphene. The SCG cover is capable of isolating CuNWs from the Cu etching solution to retain the intact sandwich structure of SCG/CuNW/UVR. Also, the embedding of CuNWs in UVR can reduce shape fluctuation and build an ultra-smooth uniform surface of SCG/CuNW/UVR electrodes. As a proof-of-principle, the SCG/CuNW/UVR TCEs showed excellent conductive-transparent properties (comparable to ITO electrode) and mechanical robust, as well as high anti-oxidation stability ($\Delta R/R_0 < 0.2$ within 180 days) and acid corrosion resistance. By employing the SCG/CuNW/UVR films as the transparent electrodes, furthermore, the flexible triboelectric nanogenerators (TENG) and quantum dot light emitting diodes (QLED) were successfully demonstrated, respectively.

## 2. Experimental method

### 2.1. Synthesis of copper nanowires

In a typical synthetic process of CuNWs, cupric chloride dehydrate (Aladdin, 99.99%), 1-hexadecylamine (Aladdin, 90%) and glucose (Kermel) were dissolved in deionized water and stirred for 8 h at room temperature to obtain a blue emulsion. The homogeneous emulsion was then transferred into a Teflon-lined autoclave and kept at 120 °C for 18 h. After reaction, chloroform was added to the as-synthesized reddish brown solution at the volume ratio of 3:1 to extract CuNWs. The red brown precipitation was separated from chloroform by centrifugation at 6000 rpm and re-dispersed in the solution of polyvinylpyrrolidone (PVP) (Aladdin, $M_w = 58000$) in ethanol or isopropanol. To remove excess PVP and traces of chloroform, CuNWs were centrifuged at 7000 rpm and then rinsed twice with ethanol.

### 2.2. Fabrication of hybrid graphene/copper nanowire electrodes

The SCG film ($R_{sh} \sim 300\ \Omega\ sq^{-1}$) was grown on single-crystal Cu (111) annealed from the commercial polycrystalline foils (25 μm thick, 99.8%, Sichuan Oriental Stars Trading Co. Ltd.) at 1030 °C by an atmospheric pressure CVD process with the mixture of $CH_4$ and $H_2$. After that, the as-synthesized CuNW ink was sprayed onto the SCG/Cu(111) foil at 110 °C using an airbrush with a distance of 13 cm from the nozzle (0.3 mm in diameter, spraying pressure: 0.2 MPa) to the foil. Subsequently, the CuNWs/SCG/Cu(111) was dipped in glacial acetic acid (Aladdin) and HCl (1 M) solution in 2 min and 15 s, respectively, in order to remove surfactant and surface oxide layer. A UV-curable resin (Norland Optical Adhesive (NOA 63), Norland Products Inc.) was then blade-coated onto the surface of CuNW/SCG/Cu(111) substrates. The NOA63 wet film was of 500 μm in thickness and cured under 365 nm UV irradiation at 48 W for 1.5 h at room temperature. Finally, the underlying copper foil was etched away using a ferric trichloride solution (2 M in deionized water), and the sandwich-structured SCG/CuNW/UVR film was obtained after ethanol washing and $N_2$ gas drying. A polycrystalline graphene film was grown and subsequently integrated with the copper nanowire network by the similar method for comparison.

### 2.3. Characterization

The sheet resistance ($R_{sh}$) was measured using a four-point square resistance tester with a digital multimeter. The Raman spectrum was measured using a Renishaw inVia microscope with a 532 nm excitation laser. The optical, transmission electron spectroscopy (TEM), scanning electron spectroscopy (SEM) and atomic force microscopy (AFM) images were recorded using an upright microscope (PSM-1000, Motic), a transmission electron microscope (JEOL, JEM-2100), a scanning electron microscope (Nova NanoSEM 450, FEI) and an atomic force microscope (Dimension Icon, Bruker), respectively. The high-resolution TEM (HRTEM) characterization was conducted on a special aberration corrected transmission electron microscope (FEI Titan 80–300). The transmittance spectrum was obtained by UV–vis spectrophotometer (PE Lambda 950, PerkinElmer).

### 2.4. Flexible TENG and QLED devices

In order to build a TENG, an electrode of silver nanowire network embedded in polyimide (AgNWs/PI) was firstly fabricated, and the AgNWs/PI electrode ($7.5 \times 2.5\ cm^2$, 6–8 $\Omega\ sq^{-1}$) was then placed onto the SCG/CuNW/UVR electrode ($7.5 \times 2.5\ cm^2$, 9–11 $\Omega\ sq^{-1}$). The conductive sides of these two electrodes were stucked to copper wire electrodes with silver glue, respectively, and the opposite insulating sides were stitched together with adhesive tape to ensure the good contact. TENG test was conducted in air at room temperature. The open-circuit voltage was measured by Keithley 6514 system electrometer, and the short-circuit current was measured by SR570 low noise current amplifier (Stanford Research System).

The QLED device was fabricated based on the layer-by-layer spin-coating of various functional materials. A solution of PEDOT: PSS (Heraeus, AI 4083) was firstly mixed with the fluorine non-ionic surfactant of Capstone® FS-31 (Dupont) with a volume ratio of 5.5% to match the wettability between graphene layer and PEDOT: PSS. And then the mixture as a hole injection layer (HIL) was spin-cast onto the SCG/CuNW/UVR film at 4000 rpm in 60 s. The PEDOT:PSS film was baked at 50 °C for 5 min in air. Subsequently, the film was transferred into the $N_2$ filled glove box and annealed at 100 °C for 10 min. A hole transport layer (HTL) of TFB (American Dye Source, Inc., 8 mg $mL^{-1}$, chlorobenzene), an active layer of quantum dots (18 mg $mL^{-1}$, toluene) and an electrode transport layer (ETL) of ZnO nanoparticles (30 mg $mL^{-1}$, ethanol) was in turn spin-coated at 3000 rpm and annealed at 100 °C, respectively. Finally, the aluminum electrode (100 nm) was deposited by e-beam evaporation. The characteristics of current-voltage,

luminance-voltage and electroluminescence were collected with a Keithley 2400 Source Meter and a Photo-research PR735 spectrometer.

## 3. Results and discussion

### 3.1. Preparation of SCG/CuNW/UVR film

The LbL preparation process of SCG/CuNW/UVR film is schematically illustrated in Fig. 1a. First, single-crystal Cu (111) was obtained by thermal annealing of industrial polycrystalline Cu foil and served as the substrate to epitaxially grow graphene. Single-crystal Cu (111) is free of grain boundaries (inducing deep thermal grooves) and step bunches, and thus has a very smooth surface (Figs. S1a–b), showing a uniform lighter color compared with that of polycrystals after slight oxidation (Fig. 1b). Well-aligned graphene domains can be grown on Cu (111) and then stitched seamlessly to form a continuous SCG film (Fig. 1c). The low energy electron diffraction (LEED), Raman spectra and 2D mapping, as well as HRTEM characterizations over the large-area SCG film indicate its monolayer and single crystal nature (Fig. 1d and Figs. S1c–d).

The CuNW network was spray-coated on the SCG/Cu (111) using a disperse solution of CuNWs. The CuNWs were prepared by a scalable hydrothermal synthesis method modified from the previous report [47] and had a twin-crystal structure with an average diameter of ~30 nm (Fig. S2). Then the NOA63 film was blade-coated and subsequently UV-cured on the dried CuNW/SCG/Cu (111) surface (Fig. 1e and Fig. S3). After removing the Cu (111) foil by chemical etching, the 4-inch sandwich-structured SCG/CuNW/UVR film was finally obtained (Fig. 1f). The SEM images reveal a randomly interweaved CuNW network encapsulated between SCG and UVR, and the CuNWs are surface-embedded onto the UVR film (Fig. 1g). The fabricated SCG/CuNW/UVR film possesses very smooth surface with root-mean-square surface roughness (RMS) of 1.85 nm, as analyzed by AFM (Fig. 1h), which is comparable to that of the commercial ITO film (RMS of 1.64 nm, Fig. S4). Such ultrasmooth surface benefits from the synergistic and intact encapsulation of CuNWs network by SCG and UVR. This structure design can also avoid protuberances even tips that give rise to the short circuit and breakdown of CuNWs based electrode, and is crucial for fabricating solution-proceed optoelectronic devices (Fig. S5).

### 3.2. Performance of SCG/CuNW/UVR electrode

We systematically probed the optical and electrical properties of SCG/CuNW/UVR film. The sheet resistance and transmittance of SCG/CuNW/UVR electrodes can be tailored by the cycling spray deposition of CuNWs on SCG (Fig. 2a–b). With 3 cycles of CuNWs deposition, the sheet resistance of SCG/CuNW/UVR film was detected to be 19 ± 1.5 Ω $sq^{-1}$ under the transmittance of 84.3% at 550 nm, which is comparable to that of commercial ITO film ($R_{sh}$ = 18 Ω $sq^{-1}$,$T_{550\ nm}$ = 85.8%). Furthermore, the optical transmittances of SCG/CuNW/UVR films were almost unabated and high in the near-infrared regions, essential for broadband optoelectronic devices. In addition, the SCG/CuNW/UVR electrode with an area of 3 × 3 $cm^2$ exhibited high conductivity and homogeneity, the sheet resistances of which revealed a mean value of 19.25 Ω $sq^{-1}$ and a standard deviation of 0.56 Ω $sq^{-1}$ (Fig. 2c). Furthermore, the conductive-AFM (C-AFM) analysis was applied to probe the electrical uniformity of film. In the contact mode, for the graphene covered CuNWs, the current was large and current distribution was uniform on the entire surface, indicating that the SCG covers voids within the CuNW network, and thus greatly improves the electrical homogeneity of the composite electrode (Fig. S6). In contrast, in the case of CuNWs partially embedded in polymer surface, only the CuNWs exhibited better electronic conductivity.

The deformation tolerance of electrode is also a critical factor for flexible electronic devices. The flexible transparent conductive SCG/CuNW/UVR film can serve as an electrode for LED lighting even if strongly bent and twisted (Fig. 2d). Furthermore, we probed the electronic properties of SCG/CuNW/UVR electrodes under bending condition. The SCG/CuNW/UVR electrode retained high conductivity even if the bending radius was up to 1 mm ($\Delta R/R_0 \leq 0.18$) (see Video S1), while the $\Delta R/R_0$ value of CuNWs/UVR electrode increased to 0.75 at the bending radius of 1 mm (Fig. 2e). Besides, the SCG/CuNW/UVR

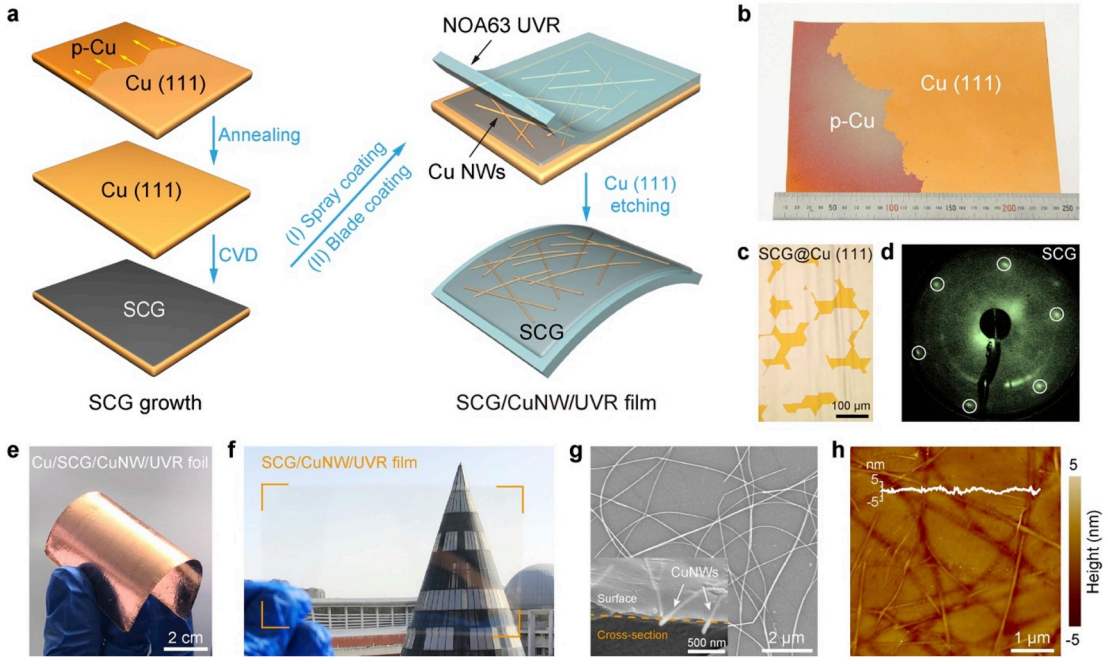


**Fig. 1.** (a) Schematic of preparation procedure of SCG/CuNW/UVR film. (b) Photograph of a single-crystal Cu (111) foil with light color on the right. (c) Optical image of aligned SCG domains on Cu (111) substrate. (d) LEED patterns of SCG film. (e, f) Photographs of Cu/SCG/CuNW/UVR foil and SCG/CuNW/UVR composite film. (g) SEM images of the SCG/CuNW/UVR composite film. Inset: cross-section image, showing the CuNW network embedded in the UVR basement. (h) AFM image of the SCG/CuNW/UVR composite film. The white curve shows the profiled height.

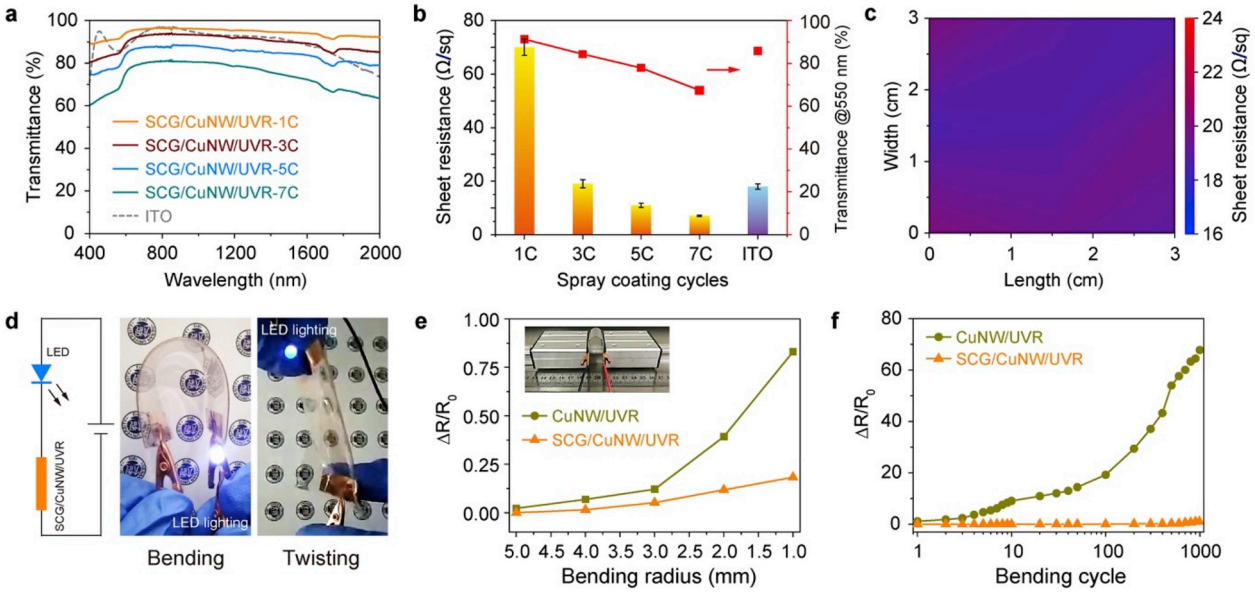


**Fig. 2.** (a–b) Visible and near-infrared transmittance spectra (a) and sheet resistances & transmittances (b) of SCG/CuNW/UVR films with different spray-coating cycles of CuNWs compared with ITO/PET film. (c) A map of sheet resistance for SCG/CuNW/UVR film with a size of 3 × 3 $cm^2$, showing good uniformity of conductivity. (d) Photographs of the bent and twisted SCG/CuNW/UVR film serving as an electrode to light up a blue LED. (e) Sheet resistance change of SCG/CuNW/UVR film over bending radius. (f) Sheet resistance change of SCG/CuNW/UVR film over bending cycle (the radius of curvature: 2.5 mm).

electrode exhibited a superior mechanical durability without obvious conductivity degradation, the $\Delta R/R_0$ value of which increased to 1 upon 1000 bend cycling, compared with the cover-free CuNW network ($\Delta R/R_0 = 135$) (Fig. 2f). It benefits from the compact covering of SCG layer on CuNW network. Such intact graphene package could also be revealed from the more highly stable conductivity of SCG/CuNW/UVR after scotch tape (3 M) peeling-off test, compared with that of the bare CuNWs electrode (Fig. S7).

Supplementary video related to this article can be found at https://doi.org/10.1016/j.nanoen.2020.104638

In general, corrosive molecules such as water and oxygen may penetrate monolayer graphene through its grain boundaries and vacancies and react with CuNWs, and this process will be accelerated by deformation under which the cracks generate easily at the defects. The SCG with perfect lattice structure can completely protect CuNWs from water and oxygen molecules, especially together with UVR, and ensure the robust stability of the CuNW network even if it was bent, twisted and stretched (Fig. 3a). We measured the aging behaviors of the bare CuNWs, CuNWs/UVR, PG/CuNW/UVR and SCG/CuNW/UVR under ambient atmosphere (Temperature: 25 °C, relative humidity: 30–70%) (Fig. 3b). The bare CuNW network failed to conduct electricity after 13 days and the CuNW network embedded in UVR also became unavailable after 30 days. The covering of PG delayed the electrode degradation, while the resistance increased up to 4.5 kΩ $sq^{-1}$ after 180 days. In contrast, the SCG/CuNW/UVR electrode had a low resistance of 17.8 Ω $sq^{-1}$ and always maintained the $\Delta R/R_0$ value less than 0.2 within half a year. According to a linear oxidation kinetics law [48], a lifetime of ~2.5 years for SCG/CuNW/UVR electrode was estimated based on the

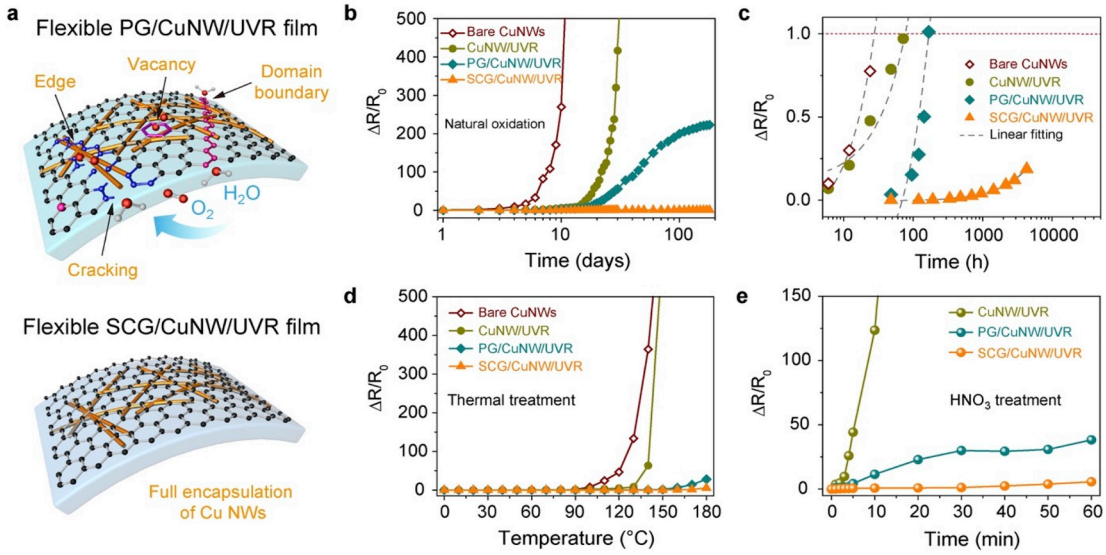


**Fig. 3.** (a) Schematic of the flexible SCG/CuNW/UVR and PG/CuNW/UVR films under ambient atmosphere. (b–e) Stability tests of bare CuNWs, CuNW/UVR, PG/CuNW/UVR and SCG/CuNW/UVR films in atmosphere environment (b–c), at elevated temperature (d) and in strong acidic solution (e). The data in (c) is extracted for $\Delta R/R_0 < 1$ from (b).

acceptable $\Delta R/R_0 = 1$ (*i. e.*, two times of sheet resistance) for most TCE applications (Fig. 3c). Furthermore, SCG/CuNW/UVR electrodes exhibited remarkable stability in much harsher environment (Fig. 3d). It showed an almost constant value of $\Delta R/R_0$ at the elevated temperature (humidity: 60%), only with a little increase above 160 °C. In contrast, the $\Delta R/R_0$ values of the bare CuNWs electrode and the embedded in UVR one drastically increased above 130 °C. The PG-covered CuNW network also showed an obvious increased resistance, from 18.6 Ω $sq^{-1}$ at room temperature to 536 Ω $sq^{-1}$ at 180 °C. Even in a solution of strong oxidizing acid (1 M $HNO_3$), the SCG/CuNW/UVR film showed a significant improvement of stability comparing to that of PG/CuNW/UVR counterpart. In such environment the CuNW/UVR electrode degraded rapidly, suggestive of the severe Cu corrosion (Fig. 3e).

To further probe the protection of SCG to CuNWs against oxidation, a sheet of SCG film was directly-contact transferred onto CuNW network with the CuNWs partially uncovered (Fig. 4a). As observed by SEM, the surface of bare CuNWs became rough after oxidation in air due to the formation of copper oxides particles and adsorbates, but the SCG covered ones remained smooth (Fig. 4b). A bundle of CuNWs partially covered with SCG was oxidized in hot air (130 °C) for 20 min (Fig. 4c). The photoluminescence (PL) spectrum was measured at the regions of bare and SCG-covered CuNWs before and after the oxidation, respectively (Fig. 4d). Note that Raman signal of the surface copper oxides on CuNWs is weak and difficult to be detected in the background of strong PL signal of CuNWs. Before oxidation, strong PL signals can be observed in both exposed regions and SCG covered regions on CuNWs, which could be related with local plasmon resonance effect of CuNWs [49]. After complete oxidation, the characteristic PL signal for CuNWs greatly decreased in exposed regions of CuNWs, indicating the formation of CuO surface [50], while the one of SCG covered CuNWs almost remained unchanged (Fig. 4e–f). These results consolidated again that the SCG could isolate the CuNWs from the water and oxygen to prevent Cu oxidation (Fig. S8).

### 3.3. Applications of SCG/CuNW/UVR electrodes

To evaluate the performance of SCG/CuNW/UVR electrodes for practical applications, a flexible transparent TENG was fabricated based on the SCG/CuNW/UVR electrode (Fig. 5a). In principle, the UVR and polyimide polymers have different triboelectric polarity in the triboelectric sequences. When the TENG was bent, the two material surfaces rubbed against each other and yielded equal and opposite charges, respectively (Fig. 5b). When the two material surfaces were separated by external force, the surface charges could flow between electrodes to form an electric current (Fig. 5c). During periodical bending and releasing processes of TENG in a cyclic agitation on the human wrist (~1 Hz, Video S2), the maximum output voltage and current signals were up to ~62 V and ~3.6 μA, respectively (Fig. 5d). This demonstration suggests the potential of SCG/CuNW/UVR electrodes for large-scale wearable electronics and smart textiles.

Supplementary video related to this article can be found at https://doi.org/10.1016/j.nanoen.2020.104638

A green QLED was assembled by a layer-by-layer spin-coating with the SCG/CuNW/UVR electrode as an anode (Fig. 5e). A gold layer was partly deposited onto the surface of SCG/CuNW/UVR film for Kelvin probe force microscopy (KPFM) analysis to evaluate the work function (Fig. S9). According to the equation $V_B - V_A = -1/e\ (\phi_B - \phi_A)$ (where V is the surface potential and ϕ is the work function), the work function of the SCG/CuNW/UVR film was calculated to be 4.87 eV. This means the faster hole injection from SCG/CuNW/UVR anode into poly(3,4-ethylenedioxythiophene)/poly(styrene sulfonate) (PEDOT:PSS) layer, compared with that from ITO anode with work function of 4.7 eV (Fig. 5f). Apparently, the SCG/CuNW/UVR-based QLED exhibited a normal lighting state even if it was bent (Fig. 5g). And its electroluminescent peak maintained stable at 530 nm when the applied drive voltage ranges from 2 to 5 V (Fig. 5h), indicating its good color purity. Furthermore, the current density-voltage characteristic curves indicate the higher current density of the SCG/CuNW/UVR-based QLED than that of the flexible ITO-based counterpart at low voltage (<1.3 V) (Fig. 5i). This could benefit from the better matching of work functions between SCG/CuNW/UVR and PEDOT: PSS and the faster hole injection at the interface. The luminance-voltage measurement (Fig. 5j) of the SCG/CuNW/UVR-based QLED shows the comparable performance to that of flexible ITO-based QLED, suggesting in return the high

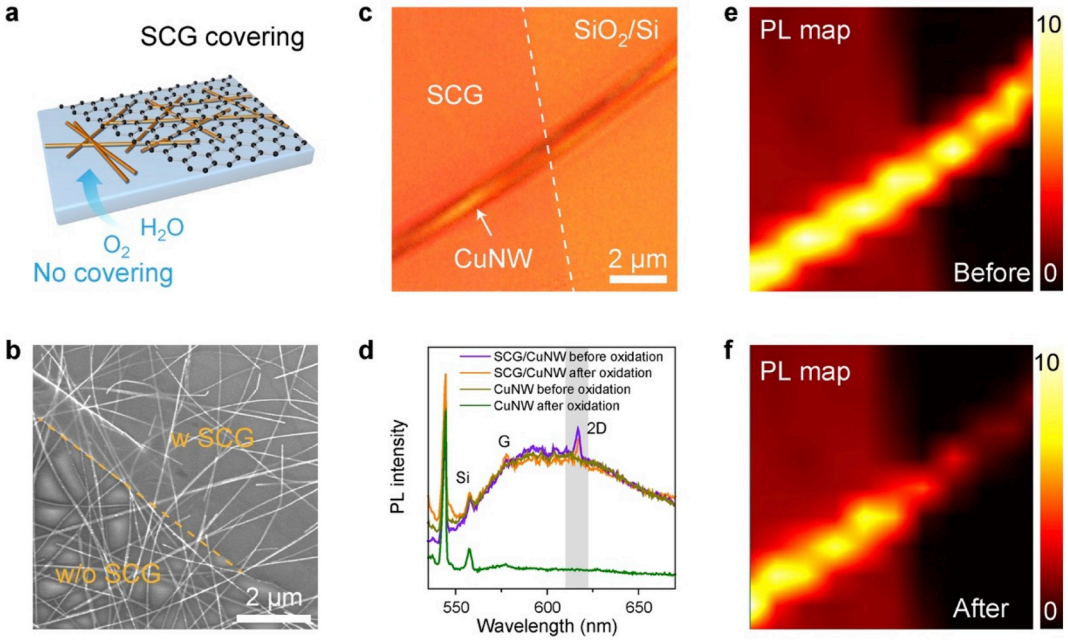


**Fig. 4.** (a) Schematic of the SCG partially covered the CuNW network. (b) SEM image of SCG/CuNW/UVR film with SCG partially covering the CuNW network. (c) Optical image of SCG partially covered a bundle of CuNWs on $SiO_2$/Si substrates. (d) Photoluminescence spectra of the bare and SCG covered CuNWs before and after oxidation, respectively. The peaks representing characteristic Raman bands from graphene (G and 2D bands) and Si substrate are presented. (e, f) PL maps of the 2D bands of graphene before (e) and after (f) oxidation.

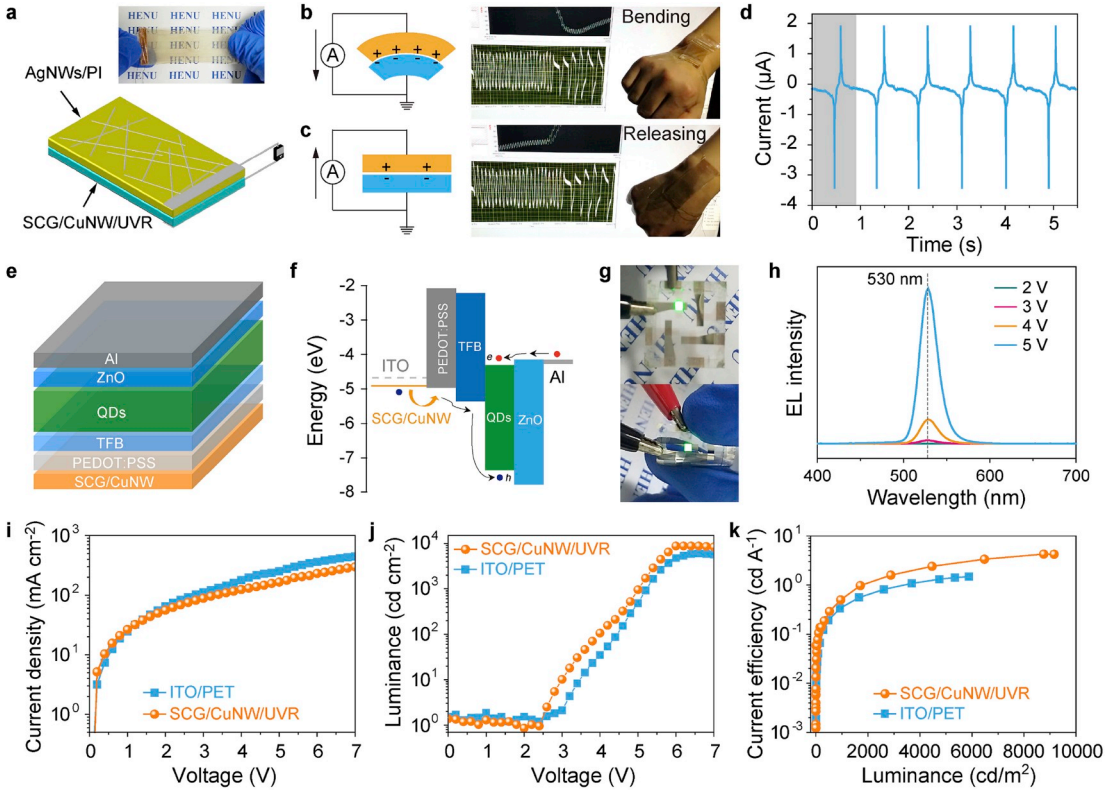


**Fig. 5.** (a) Schematic of flexible SCG/CuNW/UVR-based TENG device. Inset: real TENG device. (b, c) Operating principle and performance of flexible SCG/CuNW/UVR-based TENG during periodical bending and releasing process on the human wrist. (d) Short-circuit current of SCG/CuNW/UVR-based TENG. (e) Schematic of a green QLED structure with the patterned SCG/CuNW/UVR film as the anode. (f) The corresponding energy band diagram of the QLED device. (g) Photographs of the SCG/CuNW/UVR-based QLED operating at normal state (top) and bending state (down). (h) Electroluminescence spectra of the SCG/CuNW/UVR-based QLED at different driving voltages. (i–j) Characteristic curves of current density and luminance of the flexible SCG/CuNW/UVR-based QLED and ITO-based QLED over driving voltage. (k) Characteristic curves of current efficiency of the flexible SCG/CuNW/UVR-based QLED and ITO-based QLED over luminance.

conductivity of SCG/CuNW/UVR electrode ($19 \pm 1.5\ \Omega\ sq^{-1}$) and good balance of electron-hole injection. The curves of current efficiency *versus* luminance (Fig. 5k) reveal that the maximum current efficiency of SCG/CuNW/UVR-based QLED was achieved at *c.a.* 4.25 cd $A^{-1}$ at 8760 cd $m^{-2}$, which was higher than that of the flexible ITO-based QLED (1.2 cd $A^{-1}$ at 5883 cd $m^{-2}$).

## 4. Conclusion

In summary, we demonstrate a flexible transparent sandwich-structured SCG/CuNW/UVR electrode using a layer-by-layer coating approach. The SCG/CuNW/UVR electrode exhibits high conductivity and flexibility, as well as extremely improved stability. Both SCG/CuNW/UVR-based TENG and QLED devices show good performance and promising potential for practical applications. Such electrode fabrication technique is ready to be scaled-up, paving the way for the industry-level applications of CuNWs and SCG, further providing a platform for two-dimensional material based flexible electrodes towards next-generation smart wearable optoelectronics.

## Declaration of competing interest

The authors declare that they have no known competing financial interests or personal relationships that could have appeared to influence the work reported in this paper.

## CRediT authorship contribution statement

**Jianwei Wang:** Investigation, Writing - original draft. **Zhihong Zhang:** Investigation, Writing - original draft. **Shujie Wang:** Investigation, Writing - original draft. **Ruifeng Zhang:** Investigation, Writing - original draft. **Yi Guo:** Investigation, Writing - original draft. **Gang Cheng:** Investigation, Writing - original draft. **Yuzong Gu:** Investigation, Writing - original draft. **Kaihui Liu:** Conceptualization, Writing - original draft, Supervision. **Ke Chen:** Conceptualization, Writing - original draft, Supervision.

## Acknowledgements

This work was supported by NSFC (U1904193 and 61875053), Special Program for Basic Research in University of Henan Province, China (20zx010), the Science and Technology Development Project of Henan Province, China (182102210029), the Program for Innovative Research Team in Science and Technology in University of Henan Province, China (19IRTSTHN019), Zhongyuan Thousand Talents Program of Henan Province, China, Young Talents Program of Henan University, China, The Key Research and Development Program of Guangdong Province, China (2019B010931001, 2018B010109009 and 2018B030327001), Bureau of Industry and Information Technology of Shenzhen, China (Graphene platform 201901161512) and China Postdoctoral Science Foundation, China (2019M660282).

## Appendix A. Supplementary data

Supplementary data to this article can be found online at https://doi.org/10.1016/j.nanoen.2020.104638.

## References


[1] W.S. Wong, A. Salleo, Flexible Electronics: Materials and Applications, Springer, New York, 2009.
[2] H.R. Lim, H.S. Kim, R. Qazi, Y.T. Kwon, J.W. Jeong, W.H. Yeo, Advanced soft materials, sensor integrations, and applications of wearable flexible hybrid electronics in healthcare, energy, and environment, Adv. Mater. (2019) 1901924.
[3] S.Y. Huang, Y. Liu, Y. Zhao, Z.F. Ren, C.F. Guo, Flexible electronics: stretchable electrodes and their future, Adv. Funct. Mater. 29 (2019) 1805924.
[4] S.R. Ye, A.R. Rathmell, Z.F. Chen, I.E. Stewart, B.J. Wiley, Metal nanowire networks: the next generation of transparent conductors, Adv. Mater. 26 (2014) 6670–6687.
[5] H.L. Peng, W.H. Dang, J. Cao, Y.L. Chen, W. Wu, W.S. Zheng, H. Li, Z.X. Shen, Z. F. Liu, Topological insulator nanostructures for near-infrared transparent flexible electrodes, Nat. Chem. 4 (2012) 281–286.
[6] Y.J. Ge, X.D. Duan, M. Zhang, L. Mei, J.W. Hu, W. Hu, X.F. Duan, Direct room temperature welding and chemical protection of silver nanowire thin films for high performance transparent conductors, J. Am. Chem. Soc. 140 (2018) 193–199.
[7] L.B. Hu, H.S. Kim, J.Y. Lee, P. Peumans, Y. Cui, Scalable coating and properties of transparent, flexible, silver nanowire electrodes, ACS Nano 4 (2010) 2955–2963.
[8] H. Wu, D.S. Kong, Z.C. Ruan, P.C. Hsu, S. Wang, Z.F. Yu, T.J. Carney, L.B. Hu, S. H. Fan, Y. Cui, A transparent electrode based on a metal nanotrough network, Nat. Nanotechnol. 8 (2013) 421–425.
[9] P.C. Hsu, D.S. Kong, S. Wang, H.T. Wang, A.J. Welch, H. Wu, Y. Cui, Electrolessly deposited electrospun metal nanowire transparent electrodes, J. Am. Chem. Soc. 136 (2014) 10593–10596.
[10] J.J. Liang, L. Li, X.F. Niu, Z.B. Yu, Q.B. Pei, Elastomeric polymer light-emitting devices and displays, Nat. Photon. 7 (2013) 817–824.
[11] Q.T. Zhou, J.N. Kim, K.W. Han, S.W. Oh, S. Umrao, E.J. Chae, I.K. Oh, Integrated dielectric-electrode layer for triboelectric nanogenerator based on Cu nanowire-Mesh hybrid electrode, Nano Energy 59 (2019) 120–128.
[12] X.W. Liang, T. Zhao, W. Jiang, X.C. Yu, Y.G. Hu, P.L. Zhu, H.R. Zheng, R. Sun, C. P. Wong, Highly transparent triboelectric nanogenerator utilizing in-situ chemically welded silver nanowire network as electrode for mechanical energy harvesting and body motion monitoring, Nano Energy 59 (2019) 508–516.
[13] H. Jang, Y.J. Park, X. Chen, T. Das, M.S. Kim, J.H. Ahn, Graphene-based flexible and stretchable electronics, Adv. Mater. 28 (2016) 4184–4202.
[14] K.S. Kim, Y. Zhao, H. Jang, S.Y. Lee, J.M. Kim, K.S. Kim, J.H. Ahn, P. Kim, J. Y. Choi, B.H. Hong, Large-scale pattern growth of graphene films for stretchable transparent electrodes, Nature 457 (2009) 706–710.
[15] S. Bae, H. Kim, Y. Lee, X.F. Xu, J.S. Park, Y. Zheng, J. Balakrishnan, T. Lei, H. R. Kim, Y.I. Song, Y.J. Kim, K.S. Kim, B. Ozyilmaz, J.H. Ahn, B.H. Hong, S. Iijima, Roll-to-roll production of 30-inch graphene films for transparent electrodes, Nat. Nanotechnol. 5 (2010) 574–578.
[16] B.W. Wang, S. Jiang, Q.B. Zhu, Y. Sun, J. Luan, P.X. Hou, S. Qiu, Q.W. Li, C. Liu, D. M. Sun, H.M. Cheng, Continuous fabrication of meter-scale single-wall carbon nanotube films and their use in flexible and transparent integrated circuits, Adv. Mater. 30 (2018) 1802057.
[17] S. Jiang, P.X. Hou, M.L. Chen, B.W. Wang, D.M. Sun, D.M. Tang, Q. Jin, Q.X. Guo, D.D. Zhang, J.H. Du, K.P. Tai, J. Tan, E.I. Kauppinen, C. Liu, H.M. Cheng, Ultrahigh-performance transparent conductive films of carbon-welded isolated single-wall carbon nanotubes, Sci. Adv. 4 (2018), eaap9264.
[18] J.H. Du, S.F. Pei, L.P. Ma, H.M. Cheng, Carbon nanotube- and graphene- based transparent conductive films for optoelectronic devices, Adv. Mater. 26 (2014) 1958–1991.
[19] J. Park, H. Yoon, G. Kim, B. Lee, S. Lee, S. Jeong, T. Kim, J. Seo, S. Chung, Y. Hong, Highly Customizable all solution-processed polymer light emitting diodes with inkjet printed ag and transfer printed conductive polymer electrodes, Adv. Funct. Mater. 29 (2019) 1902412.
[20] Y.H. Kim, J. Lee, S. Hofmann, M.C. Gather, L. Muller-Meskamp, K. Leo, Achieving high efficiency and improved stability in ITO-free transparent organic light-emitting diodes with conductive polymer electrodes, Adv. Funct. Mater. 23 (2013) 3763–3769.
[21] W.W. Xiong, H.L. Liu, Y.Z. Chen, M.L. Zheng, Y.Y. Zhao, X.B. Kong, Y. Wang, X. Q. Zhang, X.Y. Kong, P.F. Wang, L. Jiang, Highly conductive, air-stable silver nanowire@iongel composite films toward flexible transparent electrodes, Adv. Mater. 28 (2016) 7167.
[22] G.F. Cai, P. Darmawan, M.Q. Cui, J.X. Wang, J.W. Chen, S. Magdassi, P.S. Lee, Highly stable transparent conductive silver grid/PEDOT:PSS electrodes for integrated bifunctional flexible electrochromic supercapacitors, Adv. Energy Mater. 6 (2016) 1501882.
[23] S. Cho, S. Kang, A. Pandya, R. Shanker, Z. Khan, Y. Lee, J. Park, S.L. Craig, H. Ko, Large-area cross-aligned silver nanowire electrodes for flexible, transparent, and force-sensitive mechanochromic touch screens, ACS Nano 11 (2017) 4346–4357.
[24] Z.Q. Niu, F. Cui, E. Kuttner, C.L. Xie, H. Chen, Y.C. Sun, A. Dehestani, K. Schierle-Arndt, P.D. Yang, Synthesis of silver nanowires with reduced diameters using benzoin-derived radicals to make transparent conductors with high transparency and low haze, Nano Lett. 18 (2018) 5329–5334.
[25] F. Cui, Y. Yu, L.T. Dou, J.W. Sun, Q. Yang, C. Schildknecht, K. Schierle-Arndt, P. D. Yang, Synthesis of ultrathin copper nanowires using tris(trimethylsilyl)silane for high-performance and low-haze transparent conductors, Nano Lett. 15 (2015) 7610–7615.
[26] Z. Zhong, H. Lee, D. Kang, S. Kwon, Y.M. Choi, I. Kim, K.Y. Kim, Y. Lee, K. Woo, J. Moon, Continuous patterning of copper nanowire-based transparent conducting electrodes for use in flexible electronic applications, ACS Nano 10 (2016) 7847–7854.
[27] J.Z. Song, J.H. Li, J.Y. Xu, H.B. Zeng, Superstable transparent conductive Cu@ $Cu_4Ni$ nanowire elastomer composites against oxidation, bending, stretching, and twisting for flexible and stretchable optoelectronics, Nano Lett. 14 (2014) 6298–6305.
[28] H.G. Im, S.H. Jung, J. Jin, D. Lee, J. Lee, D. Lee, J.Y. Lee, I.D. Kim, B.S. Bae, Flexible transparent conducting hybrid film using a surface-embedded copper nanowire network: a highly oxidation-resistant copper nanowire electrode for flexible optoelectronics, ACS Nano 8 (2014) 10973–10979.
[29] G. Zhao, W. Wang, T.S. Bae, S.G. Lee, C. Mun, S. Lee, H.S. Yu, G.H. Lee, M. Song, J. Yun, Stable ultrathin partially oxidized copper film electrode for highly efficient flexible solar cells, Nat. Commun. 6 (2015) 8830.
[30] S.J. Kwon, T.H. Han, T.Y. Ko, N. Li, Y. Kim, D.J. Kim, S.H. Bae, Y. Yang, B.H. Hong, K.S. Kim, S. Ryu, T.W. Lee, Extremely stable graphene electrodes doped with macromolecular acid, Nat. Commun. 9 (2018) 2037.
[31] J. Lee, T.H. Han, M.H. Park, D.Y. Jung, J. Seo, H.K. Seo, H. Cho, E. Kim, J. Chung, S.Y. Choi, T.S. Kim, T.W. Lee, S. Yoo, Synergetic electrode architecture for efficient graphene-based flexible organic light-emitting diodes, Nat. Commun. 7 (2016) 11791.
[32] Z.Y. Liu, K. Parvez, R.J. Li, R.H. Dong, X.L. Feng, K. Mullen, Transparent conductive electrodes from graphene/pedot:pss hybrid inks for ultrathin organic photodetectors, Adv. Mater. 27 (2015) 669–675.
[33] B. Deng, P.C. Hsu, G.C. Chen, B.N. Chandrashekar, L. Liao, Z. Ayitimuda, J.X. Wu, Y.F. Guo, L. Lin, Y. Zhou, M. Aisijiang, Q. Xie, Y. Cui, Z.F. Liu, H.L. Peng, Roll-to-roll encapsulation of metal nanowires between graphene and plastic substrate for high-performance flexible transparent electrodes, Nano Lett. 15 (2015) 4206–4213.
[34] A.G. Ricciardulli, S. Yang, G.J.A.H. Wetzelaer, X.L. Feng, P.W.M. Blom, Hybrid silver nanowire and graphene-based solution-processed transparent electrode for organic optoelectronics, Adv. Funct. Mater. 28 (2018) 1706010.
[35] F. Zhou, Z.T. Li, G.J. Shenoy, L. Li, H.T. Liu, Enhanced room-temperature corrosion of copper in the presence of graphene, ACS Nano 7 (2013) 6939–6947.
[36] M. Schriver, W. Regan, W.J. Gannett, A.M. Zaniewski, M.F. Crommie, A. Zettl, Graphene as a long-term metal oxidation barrier: worse than nothing, ACS Nano 7 (2013) 5763–5768.
[37] X.Z. Xu, D. Yi, Z.C. Wang, J.C. Yu, Z.H. Zhang, R.X. Qiao, Z.H. Sun, Z.H. Hu, P. Gao, H.L. Peng, Z.F. Liu, D.P. Yu, E.G. Wang, Y. Jiang, F. Ding, K.H. Liu, Greatly enhanced anticorrosion of cu by commensurate graphene coating, Adv. Mater. 30 (2018) 1702944.
[38] A. Aliprandi, T. Moreira, C. Anichini, M.A. Stoeckel, M. Eredia, U. Sassi, M. Bruna, C. Pinheiro, C.A.T. Laia, S. Bonacchi, P. Samori, Hybrid copper-nanowire-reduced-graphene-oxide coatings: a "green solution" toward highly transparent, highly conductive, and flexible electrodes for (opto)electronics, Adv. Mater. 29 (2017) 1703225.
[39] S.Y. Huang, Q.Z. Zhang, P.D. Li, F.Q. Ren, A. Yurtsever, D.L. Ma, High-performance suspended particle devices based on copper-reduced graphene oxide core-shell nanowire electrodes, Adv. Energy Mater. 8 (2018) 1703658.
[40] R. Mehta, S. Chugh, Z.H. Chen, Enhanced electrical and thermal conduction in graphene-encapsulated copper nanowires, Nano Lett. 15 (2015) 2024–2030.
[41] Y. Ahn, Y. Jeong, D. Lee, Y. Lee, Copper nanowire-graphene core-shell nanostructure for highly stable transparent conducting electrodes, ACS Nano 9 (2015) 3125–3133.
[42] R.K. Joshi, P. Carbone, F.C. Wang, V.G. Kravets, Y. Su, I.V. Grigorieva, H.A. Wu, A. K. Geim, R.R. Nair, Precise and ultrafast molecular sieving through graphene oxide membranes, Science 343 (2014) 752–754.
[43] H. Wang, X.Z. Xu, J.Y. Li, L. Lin, L.Z. Sun, X. Sun, S.L. Zhao, C.W. Tan, C. Chen, W. H. Dang, H.Y. Ren, J.C. Zhang, B. Deng, A.L. Koh, L. Liao, N. Kang, Y.L. Chen, H. Q. Xu, F. Ding, K.H. Liu, H.L. Peng, Z.F. Liu, Surface monocrystallization of copper foil for fast growth of large single-crystal graphene under free molecular flow, Adv. Mater. 28 (2016) 8968–8974.
[44] V.L. Nguyen, D.J. Perello, S. Lee, C.T. Nai, B.G. Shin, J.G. Kim, H.Y. Park, H. Y. Jeong, J. Zhao, Q.A. Vu, S.H. Lee, K.P. Loh, S.Y. Jeong, Y.H. Lee, Wafer-scale single-crystalline AB-stacked bilayer graphene, Adv. Mater. 28 (2016) 8177–8183.
[45] B. Den, Z.W. Xin, R.W. Xue, S.S. Zhang, X.Z. Xu, J. Gao, J.L. Tang, Y. Qi, Y. N. Wang, Y. Zhao, L.Z. Sun, H.H. Wang, K.H. Liu, M.H. Rummeli, L.T. Weng, Z. T. Luo, L.M. Tong, X.Y. Zhang, C.S. Xie, Z.F. Liu, H.L. Peng, Scalable and ultrafast epitaxial growth of single-crystal graphene wafers for electrically tunable liquid-crystal microlens arrays, Sci. Bull. 64 (2019) 659–668.
[46] X.Z. Xu, Z.H. Zhang, J.C. Dong, D. Yi, J.J. Niu, M.H. Wu, L. Lin, R.K. Yin, M.Q. Li, J. Y. Zhou, S.X. Wang, J.L. Sun, X.J. Duan, P. Gao, Y. Jiang, X.S. Wu, H.L. Peng, R. S. Ruoff, Z.F. Liu, D.P. Yu, E.G. Wang, F. Ding, K.H. Liu, Ultrafast epitaxial growth of metre-sized single-crystal graphene on industrial Cu foil, Sci. Bull. 62 (2017) 1074–1080.
[47] F. Qian, P.C. Lan, T. Olson, C. Zhu, E.B. Duoss, C.M. Spadaccini, T.Y.J. Han, Multiphase separation of copper nanowires, Chem. Commun. 52 (2016) 11627–11630.
[48] A.R. Rathmell, M. Nguyen, M.F. Chi, B.J. Wiley, Synthesis of oxidation-resistant cupronickel nanowires for transparent conducting nanowire networks, Nano Lett. 12 (2012) 3193–3199.
[49] U. Lee, Y. Han, S. Lee, J. Suk Kim, Y.H. Lee, U.J. Kim, H. Son, Time evolution studies on strain and doping of graphene grown on a copper substrate using Raman spectroscopy, ACS Nano 14 (2020) 919–926.
[50] C.Y. Huang, A. Chatterjee, S.B. Liu, S.Y. Wu, C.L. Cheng, Photoluminescence properties of a single tapered CuO nanowire, Appl. Surf. Sci. 256 (2010) 3688–3692.